IranJOC

Iranian Journal of
Organic Chemistry

Synthesis and characterization of a new poly (Lactic Acid)/ copper oxide/ tranexamic acid nanofibrous nanocomposite as an effective textile for wound healing process

Samira Molapour Rashedi[a], Ramin khajavi[b,*], Abosaeed Rashidi[a], Mohammad Karim Rahimi[c], Abbas Bahador[d]

[a]*Department of Textile Engineering, Science and Research Branch, Islamic Azad University, Tehran, Iran*
[b]*Department of Polymer and Textile Engineering, South Tehran Branch, Islamic Azad University, Tehran, Iran*
[c]*Department of Microbiology, Tehran Medical Science Branch, Islamic Azad University, Tehran, Iran*
[d]*Department of Medical Microbiology, School of Medicine, Tehran University of Medical Sciences, Tehran, Iran*

Abstract: Chronic wounds represent notable clinical problems and even impose a massive financial burden on health care systems. Textile dressings for wound care are often made up of various materials, having remarkable properties, which can help enhance wound healing process. Polylactic acid has been recognized as a useful medicine in a wide range of hemorrhagic conditions such as surgeries and chronic wounds. The present study was to describe the development of novel wound dressings of polylactic acid (PLA) nanofibers loaded with CuO NPs and TXA. The structure of the PLA/CuO/TXA nanofibrous nanocomposites (NCs) was further confirmed by the field emission scanning electron microscopy (FESEM), the energy dispersive X-ray (EDX) analysis, and the Fourier-transform infrared spectroscopy (FTIR). The antibacterial efficiency was then evaluated using both Gram-negative and Gram-positive bacteria. Besides, in vitro cytotoxicity and in vivo wound healing activity were assessed. The study results revealed that the NCs concerned not only inhibited bacterial growth but also demonstrated excellent proliferation and viability for fibroblastic cells (FCs) in injured skin.

Keywords: Wound dressings, Copper oxide nanoparticle, Tranexamic acid, Polylactic acid.

Introduction

Chronic wounds are among frequent and widespread problems that often occur throughout the human life span and even impose a massive financial burden on health care systems [1]. In recent years, active textiles for wound care and treatment have attracted researchers' attention and many different types of materials have been so far utilized in this field [2,3]. An ideal wound dressing is a non-toxic, permeable, and biocompatible covering with an antimicrobial activity, capable of protecting wounds from traumas and infections.

Recent advances in nanotechnology have also opened new routes to the applications of nanostructures in medicine [4]. For instance, nanofibrous-nanocomposite (NC) scaffolds have been prepared from various polymer matrices incorporated with nanoparticles (NPs) that play an important role in medical dressings.

Many researchers have further examined the uses of NCs in biomedical fields such as drug delivery, tissue engineering, and wound textile dressing [5]. Among various metal oxide NPs, copper (II) oxide (CuO) ones have attracted particular attention, thanks to their distinct features such as suitable redox potentials and excellent long-time stability [6]. CuO NPs have even shown excellent antimicrobial activities against various

*Corresponding author. Tel.: +98-218883310; E-mail: rkhajavi@gmail.com

bacterial strains including Gram-positive and -negative germs that can be beneficial for medical purposes and wound healing process [7]. Furthermore, nanofibers, as a great group of nanostructures used in the environment and biomedical fields, have been studied by researchers [8]. In this respect, electrospinning refers a fiber production method utilized to fabricate nanofibrous membranes from polymer solutions. The electrospun fibers with controllable diameters, ranging from nanometer (nm) to micrometer (μm) scales, also have unique properties such as high porosity, low density, large surface area, and high volume ratio [9]. These properties make them a suitable drug carrier candidate with high drug loading capacity, which enhances tissue healing and repair [10]. Moreover, electrospun nanofibers can be made from various polymers such as polylactic acid (PLA), chitosan, and cellulose acetate (CA) or their blending.

In this respect, PLA is one of the most widely used biodegradable polyesters in electrospinning applications [11]. Nanofibrous dressings made up of PLA accordingly have potential applications in regenerative medicine such as wound healing due to their excellent biocompatibility and biodegradability [12]. Drug-embedded nanofibrous scaffolds are also proper candidates for wound healing, which can be applied to regulate drug delivery in a sustainable manner. Therefore, numerous research has been so far conducted on drug-loading and release from fibers in wound dressings [13]. As well, tranexamic acid (TXA) is an antifibrinolytic drug that reduces postoperative blood losses, applied in a wide range of hemorrhagic conditions especially in surgeries and chronic wounds [14]. In this line, Sasmal et al. had investigated TXA incorporation into chitosan nanofibers to get hemostatic membranes for a broad range of clinical applications [15]. However, there is no report, to the best of authors' knowledge, on the incorporation of TXA and NPs in nanofibers in the existing literature. In this research, as the first attempt, a new PLA/CuO/TXA nanofibrous NC was introduced as an effective dressing for wound care and treatment. This structure displayed the characteristics of both electrospun nanofibers and NP additives, which could accelerate wound healing process and even solve problems occurring in conventional dressings.

Results and discussion

Characterization of PLA/CuO/TXA Nanofibrous NCs

The FESEM micrographs of the PLA/CuO/TXA nanofibrous mat (Figure **1**) showed a uniform, bead-free, and highly aligned nanofibrous morphology with an average size of 65 nm in diameter. The sphere-shaped CuO NPs were then properly incorporated inside it with an average size of 45 nm in diameter and low degree of aggregation. The FESEM image of the PLA/CuO/TXA nanofibrous NCs showed homogeneous, smooth, bead-free nanofibers with the CuO NPs properly incorporated inside them. The addition of TXA and the CuO NPs to the PLA mixture also demonstrated little effect on the uniformity of the electrospun fibers. The fibers produced in this study were randomly oriented with interconnecting pores, which enhanced oxygen permeability and allowed fluid transfer from the wound site to the dressings. The EDS was further used to characterize and confirm the prepared framework of the NCs (Figure **2**). The CuO NPs also showed characteristic peak lines around 0.94, 8.04, and 8.89 keV, which could be attributed to L_α, K_α, and K_β for Cu and 0.53 keV for K_a of O, respectively. Moreover, the EDS data of the sample indicated the characteristic emission lines of 022 keV for K_α of C. The presence of TXA in the NCs was assigned by the FTIR spectrum of the NCs (Figure **3**). The spectrum also showed an ester carbonyl stretch from the PLA at 1762 cm^{-1}. As well, (C-O), (C-H) and (NH) stretch bends of TXA were assigned at 1384, 1455, 2945, and 3504 cm^{-1}. Furthermore, the major stretching vibrations of CuO were observed at the absorption peak of 525 cm^{-1} that was in agreement with the data available in the literature [16].

Besides, the surface wettability of the mat as an essential agent in fluid absorption of wound dressings improved cell attachment for the skin cells. Figure **4** shows the contact angle values of the droplets on the surfaces of PLA/CuO/TXA nanofibrous NCs by 78°, whereas the contact angle for PLA mentioned in the literature had been 85° [17]. This value of the contact angle substantiated the hydrophilic characteristics of the structure that was due to the presence of the CuO NPs.
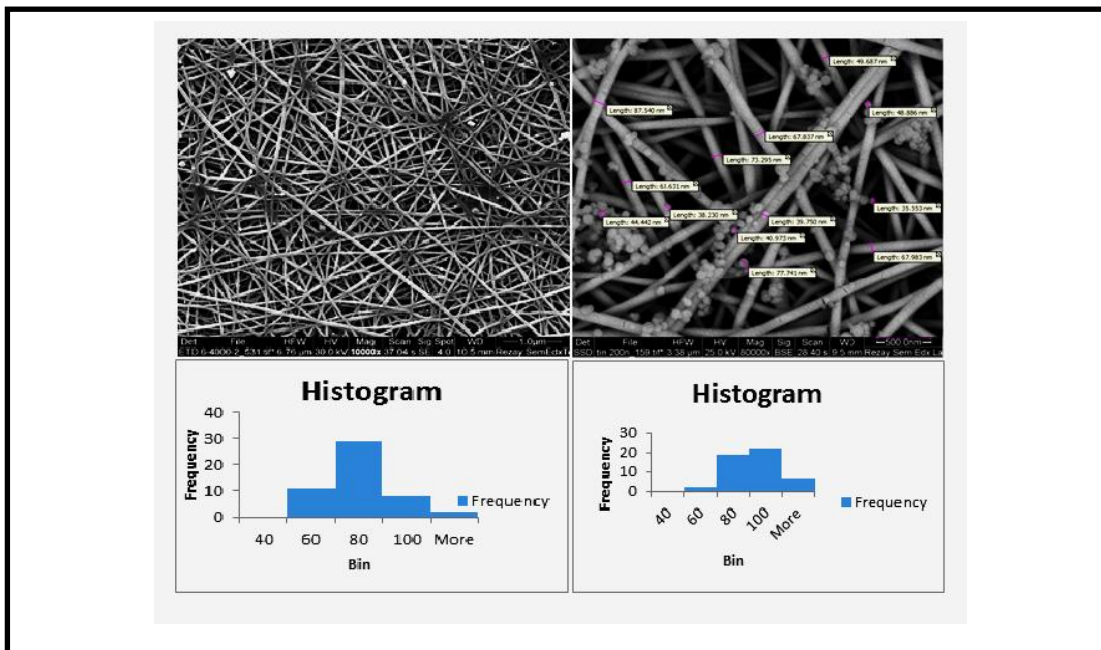
Figure 1: FESEM images of a) PLA and b)PLA/CuO/TXA nanofibrous nanocomposite
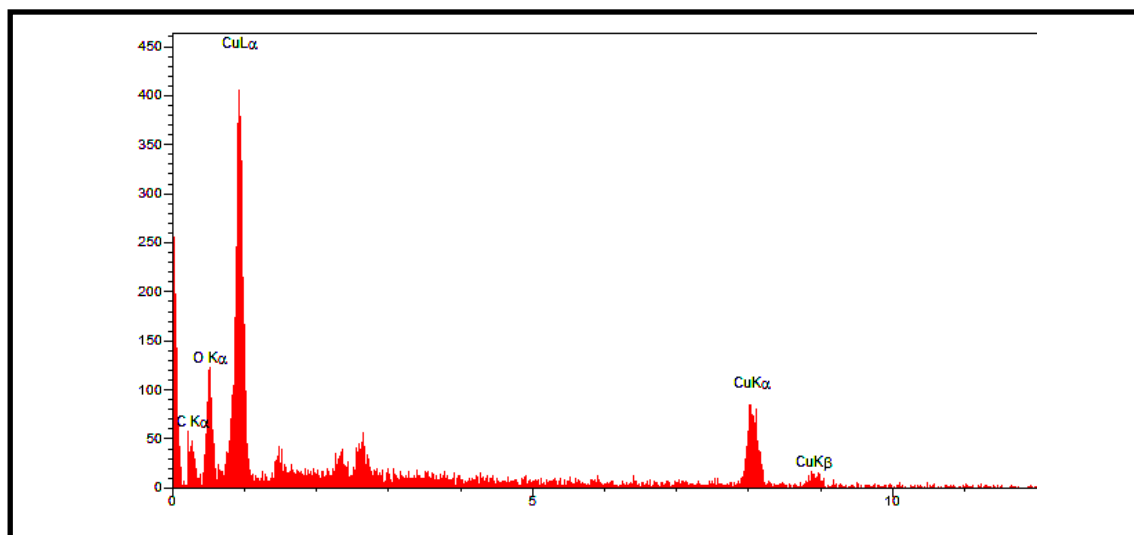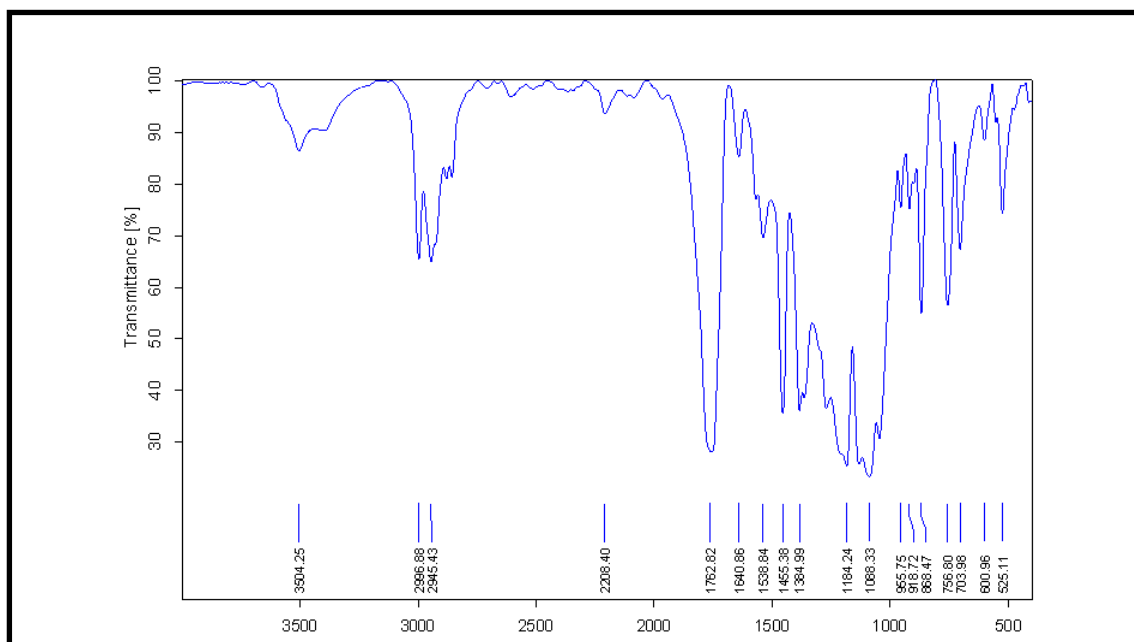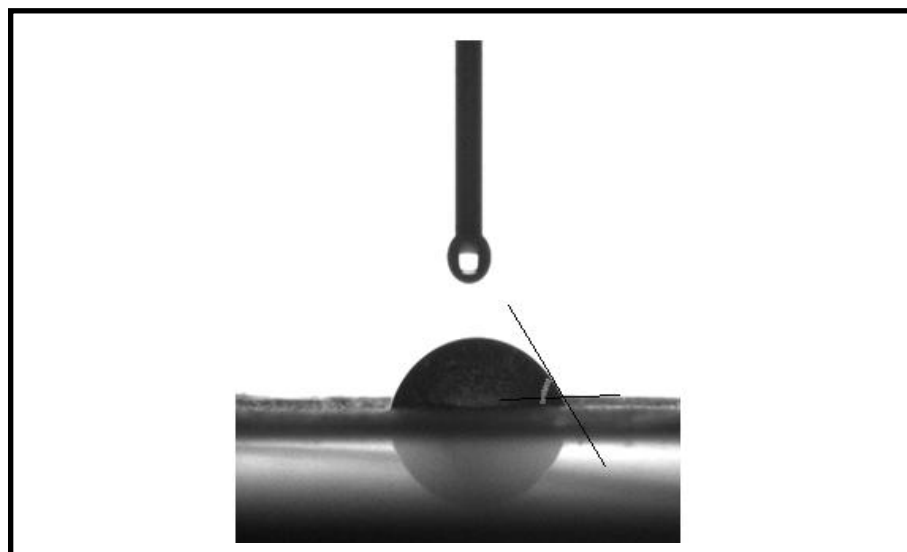

Figure 2: EDS analysis of PLA/CuO/TXA nanofibrous nanocomposites

**Figure 3.** FT-IR Spectrum of PLA/CuO/TXA nanofibrous nanocomposites

Figure 4: Water contact angle image of PLA/CuO/TXA nanofibrous nanocomposite

Antibacterial Activities

To expand the anti-bacterial activity of the NC mat, the CuO NPs were added into the spun PLA fibers. The antibacterial activity was then calculated using CFU per ml of the solution.

The R% of the bacterial growth for the PLA/CuO/TXA nanofibrous NCs against *E. coli*, *S. aureus*, *Pseudomonas aeruginosa* (*P. aeruginosa*), and *Candida albicans* (C. albicans) after 24 h with a concentration of 0.5, 1, and 2% CuO in the cultures are presented in Figure **5**.
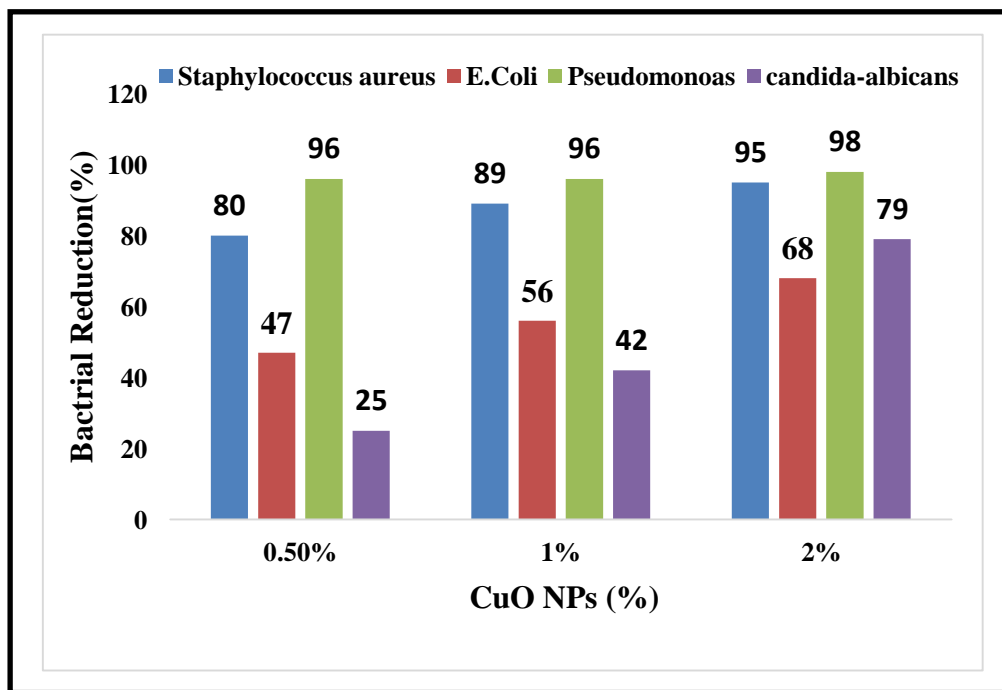
Figure 5: a) Antibacterial activity graph of PLA/CuO/TXA nanofibrous nanocomposites against four bacteria. b) Some figures of antimicrobial test.

The CuO NPs at even less concentration showed higher than 80% bacterial reduction against *P. aeruginosa* and *S. aureus* than in *E. coli* and *C. albicans*. As the concentration increased, the bacterial reduction also augmented irrespective of the type of bacteria.

Of note, *P. aeruginosa* is one of the most commonly considered aerobic bacilli that can lead to chronic wounds and infections when tissues are traumatically injured. In addition, staphylococci are a common type of bacteria that live on the skin and mucous membranes of humans so that approximately 30% of the human population is colonized with *S. aureus*, as one of the most dangerous bacteria in human diseases because it is resistant to some commonly used antibiotics. Therefore, finding a way to control pathogens commonly associated with wound infections seems necessary.

The results of this study confirmed that the CuO NPs in these dressings were an economic alternative antibacterial agent especially in treating acute infections without taking risk of developing resistant bacterial

strains as with antibiotics. A similar trend had been also observed by other researchers testing CuO-based products against different four pathogens, with specificity towards pathogenic Gram-positive bacteria [18].

The mechanism of the antibacterial activity of CuO NPs is not exactly known. The bacterial reduction can be thus explained by the penetration and adhesion of CuO NPs to the protein containing sulfur in the cell wall of the bacteria, which causes the bacterial cell death. Further production of active oxygen species, like hydrogen peroxide (H_2O_2), by CuO NPs can thus inhibit the growth of bacterial cells [19]. As the nanofibrous NCs produced in this study showed good antibacterial activity against bacteria, they can be used for infection prevention in wound healing process.

Coagulation Assay

The OD values of Hb at 540 nm for the nanofibrous NC sunder the predetermined time intervals are displayed in Figure **6**. The rate of blood coagulation was also measured by the OD values of Hb at different times. The results showed the pure PLA nanofibers and control samples had a similar curve at different time points, while the PLA/CuO nanofibrous NC mat loaded with TXA had lower OD values after being incubated for 60 min under comparable experimental conditions. Besides, a higher OD value represented a higher Hb concentration and revealed that blood coagulation was less obvious. Therefore, loading TXA in wound dressings can successfully control bleeding in chronic wounds.

In Vitro Cytotoxicity

The cytotoxic activity of the synthesized NCs was tested by means of the MTT assay against human skin FCs and MSCs. Figure **7** illustrates the fluorescence images of the FCs cultured on the PLA/CuO/TXA nanofibrous scaffolds for 3 days using the live/dead assay. The fluorescence color of the cells cultured on the PGA/CuO/TXA nanofibrous mat was totally in orange, indicating a good viability of the FCs. The MTT assay results clearly suggested that the PLA/CuO/TXA nanofibrous scaffolds provided an appropriate environment to the FCs.

Figure **7** also shows the data obtained from the MTT assay of the proliferation and viability of human skin FCs and MSCs seeded on the PLA/CuO/TXA hybrid nanofibrous scaffolds. It was observed that the FCs comfortably proliferated on the PLA/CuO/TXA nanofibrous scaffolds and cell viability was reduced to 87% and 82% respectively after 24 h. These results

clearly demonstrated that the NCs provided a cytocompatible nature for cell proliferation. The biosafety of PLA had been also approved by the United States Food and Drug Administration (FDA) for use in the human body and had been previously studied in the related literature [20].

In addition, some researchers had reflected on the toxic activity of CuO NPs towards human cells, with a special focus on skin penetration. The results had shown that the absorption of the CuO NPs through intact skin after 24 h of exposure had been insignificant, because the epidermis could act as the main barrier against the dispersion of such NPs. Moreover, the results had found an increasing permeation of Cu in damaged skin but the CuO NPs had stopped in the first skin layer.

In Vivo Wound Healing Activity

In the present study, wound healing process in mice was monitored at the time points of 0, 7, 14 days (Figure **8**). The effect of the substitution of the layers of epidermis with the PLA/CuO/TXA NC dressings in wound healing was also assessed over days. On day 7 after injury, the epidermal substitute group showed significantly better wound closure compared with the control group. After 14 days, the wound in the epidermal substitutes had achieved complete wound closure, but the wound of the control group was not completely closed. The reason for this high closure rate of the wound by the NCs was the release of TXA as an antifibrinolytic drug from the nanofibers, which had prevented the conversion of plasminogen into plasmin, inducing blood clots from wounds.

It should be noted that nanofibrous structure of mats offer several operational advantages compared with conventional wound dressings. The high specific surface areas and the enormous porosity help in the easy release of TXA drug to the wounds over a prolonged period. The narrow pore sizes in nanofibers also lead to good permeability and volatilization of tissue fluid and adjust the humidity of skin tissue. As well, nanofibrous scaffolds can promote FC adhesion and proliferation that can accelerate the re-epithelialization of skin wound [21].

Furthermore, the antibacterial activity of CuO is an important property in accelerated wound healing and inhibition of wound infections, which would result in faster wound healing. In this line, Venkataprasanna et al. had fabricated a chitosan/poly(vinyl alcohol)(PVA)/ graphene oxide (GO)/CuO patch for potential wound healing applications [22].
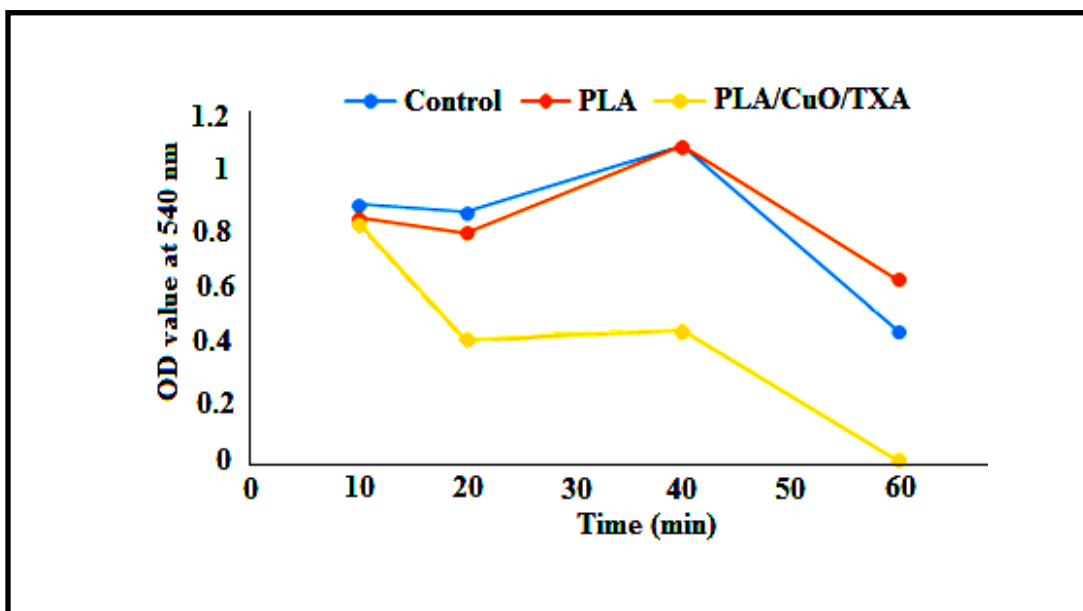
Figure 6: Coagulation assay of PLA/CuO/TXA nanofibrous nanocomposites at different time intervals
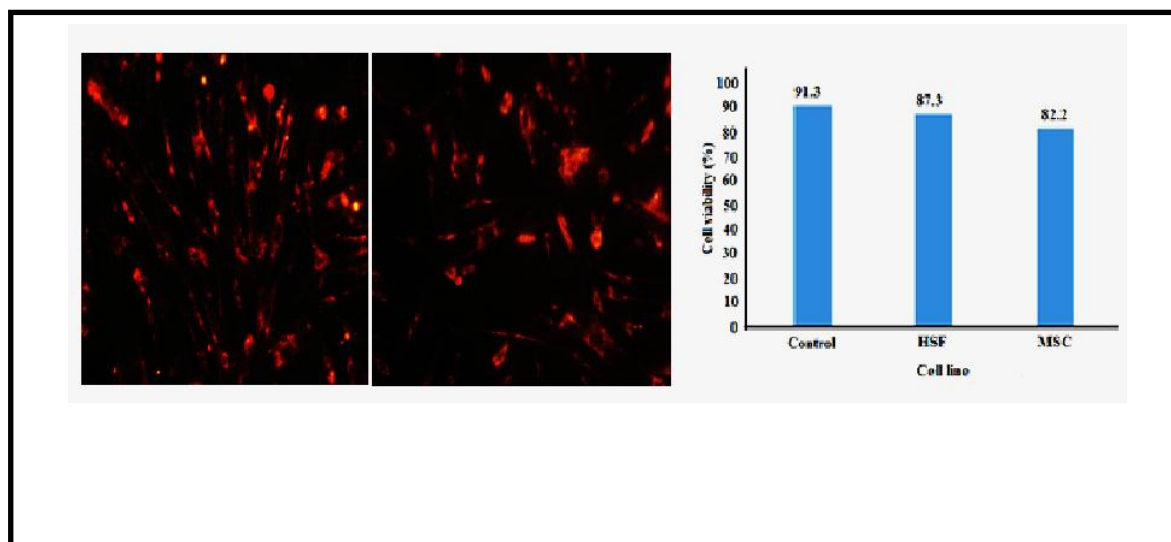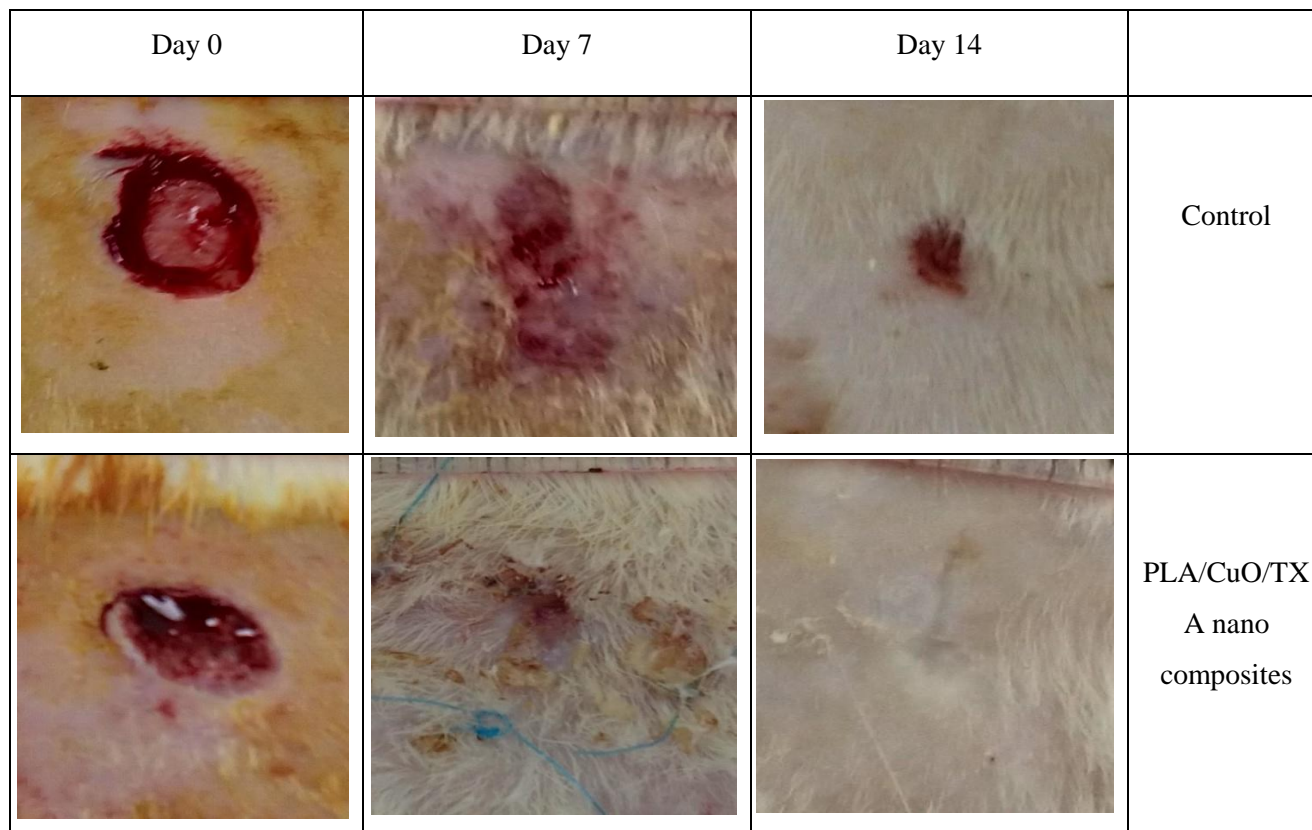

Figure 7: Fluorescence microscopy images of human fibroblast cell viability a) control group and b) in the presence of PLA/CuO/TXA nanofibrous nanocomposites, Cell viability analysis by using MTT assay , for human skin fibroblast (HSF) and Mesenchymal Stem Cell (MSC).

Day 0	Day 7	Day 14	
			Control
			PLA/CuO/TX A nano composites

Figure 8: The representative images of skin wound healing in mice after treatment with the PLA/CuO/TXA nanofibrous nanocomposites. Untreated wounds were used as controls

Conclusion

Recent developments in nanofibrous NCs and applying them in medical fields have thus far induced a significant production of new textiles especially in wound dressing process. The present study reflected on the synthesis and characterization of a new PLA/CuO/TXA nanofibrous NC as a novel wound dressing. The structure of the NCs was also characterized using the FTIR, the FESEM, and the EDS analysis and confirmed the incorporation of drug and NPs in them. The results of the blood coagulation assay also indicated that the NCs concerned could properly coagulate blood in wounds.

Furthermore, the PLA/CuO/TXA nanofibrous mat showed high antibacterial activity in the tested bacterium, which was predominantly present in the wounds. The cell viability assay concluded that the dressing had good cell viability with low toxicity and increased proliferation of FCs. The increase in cell migration and proliferation thus conformed to the potential applications of the PLA/TXA nanofiber incorporated with the CuO NPs in wound healing applications.

Thus, the fabricated PLA/CuO/TXA nanofibrous mat shows a promising way for wound healing as it inhibits bacterial growth in wounds, and helps in cell proliferation and accelerated wound healing.

Experimental

Materials

PLA (Mn=70,000-90,000), TXA, copper nitrate (Cu [NO$_3$]$_2$), sodium hydroxide (NaOH), and dichloromethane (CH$_2$Cl$_2$) were initially obtained from Sigma-Aldrich Chemicals, Munich, Germany. All the reagents were also of analytical grade and they were used without further purification. The CuO NPs were then synthesized via chemical precipitation using Cu(NO$_3$)$_2$ and NaOH as a precursor and a reducing agent, respectively [23].

The antimicrobial activity of the structure concerned was further studied against the bacterial strain including Gram-positive bacterial *Staphylococcus aureus* (*S. aureus*: ATCC 25023) and Gram-negative bacterial *Escherichia coli* (*E. coli*: PTCC 1399),

prepared from the Persian Type Culture Collection (PTCC), Tehran, Iran.

The human skin fibroblast cells (FCs) and the mesenchymal stem cells (MSCs) were also obtained from the Skin Research Center, Tehran University of Medical Sciences, Tehran, Iran. As well, 3-(4, 5-dimethylthiazol-2-yl)-2, 5-diphenyltetrazolium bromide (MTT), Dulbecco's Modified Eagle Medium (DMEM), and phosphate buffer saline (PBS) were acquired from Thermo Fisher Scientific (Waltham, MA, USA).

Preparation of PLA/CuO/TXA Nanofibrous NCs

Firstly, PLA (1 gr) was dissolved in 10 mL CH_2Cl_2 and a solution concentration of 10 wt.% was prepared. The CuO NPs (0.5, 1, 2 wt.%) and TXA (2 wt.%) were then dispersed in the PLA solution and sonicated at room temperature for 90 min to disrupt possible agglomerates.

The PLA/CuO/TXA nanofibrous mats were also produced by the electrospinning of the prepared solution using an electrospinning machine (NanoAzma, side-by-side model, Iran). The solution was consequently fed into a needle through a syringe pump. Afterwards, a voltage in the range of 10 kV was applied to the needle and the syringe pump was set at a flow rate of 0.3 mL h^{-1}. The distance tip needle-to-collector was also adjusted in 10 cm and the electrospinning process was conducted for 2 h. At the end, the nanofibrous mat was collected on an aluminum foil and peeled off for characterization.

Characterization

Field emission scanning electron microscope (FESEM, model: MIRA 3-TESCAN) was employed to obtain the size and the surface morphology of the NCs. The high-resolution FESEM images of the samples were quantitatively analyzed by the Image J software (the National Institutes of Health version 1.48v, USA). The energy-dispersive X-ray spectroscopy (EDS, model SAMx), at an accelerating voltage of 100 KV, was also used to analyze the elemental composition of the structure.

A spectrophotometer (Shimadzu, IRTracer-100 FTIR Spectrometer) at 400-4000 cm^{-1} wavelengths, was further employed for the Fourier-transform infrared spectroscopy (FTIR). As well, the sessile drop method was recruited for measuring the contact angle and the wettability of the PLA/CuO/TXA nanofibrous NCs. This method was carried out with an especially arranged microscope equipped with a camera (Canon EOS 700D) and the PCTV Vision software.

Antibacterial Activity

At first, the bacterial strains were cultivated for 24 h at 37°C in the Muller-Hinton agar. Then, a sample of the colonies was removed from the surface of the agar plate and suspended in a sterile physiological solution (0.9% sodium chloride [NaCl] at a density of $1.5×10^8$ viable colony-forming units per milliliter (CFU/mL). Afterwards, the circular discs of the nanofibrous mats (2.5×2.5cm) were kept into the bacterial solution, which was followed by incubation at 37°C. The percentage reduction (R%) of the bacterial growth was also determined according to the following equation:

$$R\ (\%) = (U-T)/U×100$$

which is based on the number of colonies formed in the petri dishes in untreated mat (U) and following treatment with the nanofibrous mat (T).

Coagulation Assay

The coagulant properties of the PLA/CuO/TXA nanofibrous mat were survived by the blood clotting test, as mentioned in the literature [24]. Firstly, a sample in a dimension of 20×20 mm of the nanofibrous mat was cut and put into an individual well of the 12-well tissue culture plat. The cover slip without nanofibers was also selected as the control. Then, 0.2 mL of human blood sample was taken and dropped onto the surface of the samples. Finally, 1 mL of calcium chloride ($CaCl_2$) solution (0.5 M) was added to each blood drop and incubated at 37°C for 1 h. The hemoglobin (Hb) absorbance values were also monitored at 540 nm, using a Jenway Model 7315 UV/Visible spectrophotometer.

In Vitro Cytotoxicity

The cytotoxicity evaluation of the nanofibrous NC was performed via the 3-(4, 5-dimethylthiazolyl-2)-2, 5-diphenyltetrazolium bromide (MTT) assay, as described in the literature [25]. First, the punched nanofibrous NC samples (1x1 cm pieces) were sterilized with ultraviolet (UV) light and placed into 96 well plates. The human normal FCs (100 μl) at a density of $6×10^4$ cells/well were then seeded into a 96-well plate in the complete growth culture medium containing DMEM, 10% PBS, and 1% penicillin-streptomycin, and were incubated for 24 h. Subsequently, 10 μL of MTT reagent was added to each well and was further incubated for 4 h. Formazan crystals formed after 4 h in each well were also dissolved in 90% (v/v) ethanol (C_2H_5OH) for 10 min. The amount of formazan was then determined from the optical density (OD) at 570 nm using a microscan

spectrum (ElectroThermo, Milford, USA), while the wells without cells were used as blanks. The results were ultimately subjected to the MTT assay for cell viability determination.

The study results obtained were statistically analyzed through the analysis of variance (ANOVA) followed by multiple Tukey's post-hoc analysis using the GraphPad Prism 6 software (San Diego, CA, USA) at the significance level of at a least $p<0.05$.

In Vivo Studies

The in vivo wound healing was simulated recruiting 10 male mice, weighing 20-25 g. The mice were randomly assigned to two groups, treated with NC mat or gauze control, consisting of three animals in each group.

The animals were initially anesthetized with an intramuscular injection of pentobarbital (30 mg/kg). Then, the dorsal skin region of the animals was shaved, and a 2×2 cm-0.5 cm full-thickness incision was made through the dorsal skin of each mouse using sterilized surgical scissors. The corresponding nanofibrous samples were consequently sterilized by UV light, attached to the wounds of all mice except for those in the control group. Wound healing processes were further assessed on days 7 and 14.

Acknowledgement

References

[1] Zomer, H. D.; Trentin, A. G. *J. Dermatol. Sci*. **2018**, *90*, 3.

[2] Chouhan, D.; Mandal, B. B. *Acta Biomater*, **2020**, *103*, 24.

[3] Kumar, Prasanth M.; Suba, V. Reddy; Rami, B. *Indian J. Exp. Biol*. **2017**, *10*, 688.

[4] Ma, R..; Shi, L. *Giant*, **2021**, 100074.

[5] Ullah, H.; Wahid, F.; Santos, H. A.; Khan, T. *Carbohydr. Polym*. **2016**, *150*, 330.

[6] Ahamed, M.; Alhadlaq, H. A.; Khan, M. A. M.; Karuppiah, P.; Al-Dhabi, N. A. *J. Nanomater.* **2014**, 637858.

[7] Nabila, M. I.; Kannabiran, K. *Biocatal. Agric. Biotechnol*. **2018**, *15*, 56.

[8] Sabra, S.; Ragab, D. M.; Agwa, M. M.; Rohani, S. *Eur J Pharm Sci*. **2020**, *144*, 105224.

[9] Wen, P.; Zong, M-H.; Linhardt, R. J.; Feng, K.; Wu, H. *Trends Food Sci. Technol.* **2017***, 70*, 56.

[10] Kamble, P.; Sadarani, B.; Majumdar, A.; Bhullar, S. *J Drug Deliv. Sci. Technol.* **2017**, *41,*124.

[11] Tyler, B.; Gullotti, D.; Mangraviti, A.; Utsuki, T.; Brem, H. *Adv. Drug Deliv. Rev*. **2016**, *107,*163.

[12] Fentahun, A. B.; Gao, J.; Jhatial, A. K.; *Mat. Des.* **2021**, 109942.

[13] Goonoo, N.; Bhaw-Luximon, A.; Jhurry, D. *J. Biomed. Nanotech*. **2014**, *10,* 2173.

[14] Chen, H.; Chen, M. *Am. J. Emerg. Med*. **2020**, *38,* 364.

[15] Sasmal, P.; Datta, P. *J. Drug Deliv Sci. Tech.* **2019**, *52,* 559.

[16] Kayani, Z. N.; Umer, M.; Riaz, S.; Naseem, S. *J. Electron. Mater.* **2015**, *44,* 3704.

[17] Abdul Hamid, Z. *Adv. Mat. Res*. **2014**, *970,* 324.

[18] Al-Jassani, M.; Qassim Raheem, H. *Int. J. Chemtech Res*. **2017**, *10,* 818.

[19] Nithiyavathia, R.; Sundaram, S. J. *J. Infec. Publ. Health*. **2021**, *14*, 1893.

[20] Conn, R. E.; Kolstad, J. J.; Borzelleca, J. F.; Dixler, D. S.; Filer, L. J.; Ladu, B. N. *Food Chem. Toxicol*. **1995**, *33,* 273.

[21] Ambekar, R. S.; Kandasubramanian, B. *Eur. Polym. J.* **2019**, *117,* 304.

[22] Sundararajan, V.; Govindan, B.; Venkatesan, M.; Banat, F. *Int. J. Biol. Macromol*. **2019**, *143,*744.

[23] Velsankar, K.; Suganya, S.; Mithumari, P. *J. Environ. Chem. Eng.* **2021**, 106299.

[24] Zhao, Y.; Wang, S.; Guo, Q.; Shen, M.; Shi, X. *J. Appl. Polym. Sci.* **2013**, *127,*4825.

[25] Rekha, S.; Anila, E. I. *Mater. Lett.* **2019**, *236,* 637.